



Surfactant Assisted One-Pot Method for Preparation of Polyethylene-Clay Nanocomposites (PECN) and Study of their Viscoelastic Behaviour

S. SIVAKALA^{1,✉}, M.S. MANJU^{2,*} and J.D. SUDHA^{3,✉}

¹Department of Chemistry, SreeNarayana College, Chempazhanthy-695587, India

²Department of Chemical Engineering, Government Engineering College, Kozhikode-673005, India

³Chemical Sciences Division, National Institute for Interdisciplinary Science and Technology CSIR, Thiruvananthapuram-695019, India

*Corresponding author: E-mail: manjupradeep@gmail.com

Received: 4 October 2022;

Accepted: 1 December 2022;

Published online: 30 January 2023;

AJC-21121

This work demonstrates a one-pot soft template-assisted technique for developing polyethylene clay nanocomposite (PECN) using cetyltrimethylammonium bromide (CTAB) micelle as structure directing agent. Linear and shear viscosities of the composite were studied in the oscillatory and rotational modes. The effect of clay content, temperature and gallery space on the storage modulus and steady-state viscosities were analyzed. The composite exhibited enhanced storage modulus over the pristine polymer, confirming strong interaction between the clay platelet and polymer molecules. The prepared PECN showed superior thermal stability, phase transition temperature, flame retardancy and mechanical properties as compared to the conventional composite. Morphological studies using SEM and TEM also confirmed the formation of the nanocomposite. This one step surfactant-assisted emulsion method offers a broad scope in designing polymer clay nanocomposites with exciting properties and consequent applications.

Keywords: Rheology, Nanocomposites, Cetyltrimethylammonium bromide, Surfactant, Polyethylene clay, Dynamic viscosity.

INTRODUCTION

Nanostructured organic/inorganic hybrid composites have recently attracted considerable attention for enhancing material properties *via* nanoscale reinforcement in contrast to the conventional particulate filled microcomposite due to the synergistic effect of molecular-level mixing of inorganic and organic materials [1]. Polymer layered silicate (PLS) nanocomposites have been actively studied during the sixties and the early seventies [2]. Later in 1990s, researchers from Toyota reported the possibility to build a nanostructure from a polymer and an organophilic layered silicate [3].

Bentonites are naturally occurring inorganic inexpensive layered materials of 2:1 phyllosilicate having a large aspect ratio (~1000) in which thin layers of aluminium silicate organize themselves in a parallel fashion to form stacks with a regular van der Waals gap in between them called interlayer spacing or gallery [4]. In the layer region, there exists Na^+ and Ca^{2+} , which can be replaced with alkylammonium or alkylphosphonium ions rendering the clay into organophilic nature [5-8].

The new material based on Nylon-6 and organophilic montmorillonite had dramatically improved mechanical properties, barrier properties and thermal resistance compared to the pristine matrix [9,10]. Later on, researchers considered several strategies for confining the polymer chains into the clay galleries. Four main processes like exfoliation adsorptions, *in situ* intercalative polymerization, melt intercalation and template synthesis are generally considered for this process [11]. Nanocomposites were prepared from a number of other thermoplastic polymers besides polypropylene such as polyamides [12], polystyrene [13], poly(ethylene oxide) [14], poly(L-lactide) [15], poly(vinyl pyridine) [16], poly(ϵ -caprolactone) [17], poly(ethylene vinyl acetate) [18] and polyimide [19].

Exfoliation adsorption is mainly applied to synthesize polymer clay nanocomposites (PCNs) with water soluble polymers. However, this process is not suitable for hydrophobic polymers such as polyethylene and polystyrene. Therefore, a two-stage process is employed for obtaining PCN with hydrophobic polymers. In this process, clay is first subjected to organo-modification by exchanging metal cations in the galleries with

an organic quaternary ammonium salt. The second step involves blending this exfoliated/intercalated clay in presence of hydrophobic polymers *via* the melt/solution process [20].

Melt state viscoelastic properties of layered silicate-based nanocomposites have attracted significant attention because of their sensitivity to the mesoscale structure of such hybrid materials and their importance in understanding the processability of such hybrid materials [13,21-27]. The mechanical and rheological properties of PCNs are related to the microstructure, the state of dispersion, the shape and orientation of the dispersed particles and particle-particle interactions. These properties are vital in the injection and extrusion moulding of nanocomposites. Earlier reports [28-30] showed that mesoscale dispersion of clay nanolayers in the polymeric matrix could be confirmed by rheological property measurement using oscillatory/rotatory modes using a compact rheometer. Studies showed that the typical rheological response of a PCN arises from frictional interactions between the silicate layers and polymeric matrix. Also, the creep behaviour is very sensitive to the microstructural changes occurring in the nanocomposite [26].

In present work, a novel one-pot technique is reported for preparing polyethylene intercalated clay nanocomposite by ultrasonication method using polyethylene-surfactant micelles in an aqueous medium. Herein, the driving force for polymer intercalation is the entropy gained by the system through the desorption of solvent molecules, which compensates for the decrease in conformational entropy of the intercalated polymer chains. This approach has the considerable benefit of being able to produce intercalated nanocomposites based on polymers with low or even no polarity. PECNs of different clay content were prepared and melt state viscoelastic behaviours were studied. All the PECN samples were characterized by XRD, SEM, TEM and rheology techniques to study the effects of clay content, intergallery space and temperature.

EXPERIMENTAL

Low-density polyethylene (LDPE) (density 922 g/cm³ MFI 3.52 g/10 min) from Metha and Co., Mumbai, India, bentonite powder (Loba Chemie, India), with cation exchange capacity of 55 meq./100 g having the chemical formula of (Na,Ca)_{0.33}(Al_{1.67}Mg_{0.33})Si₄O₁₀(OH)₂·nH₂O, cetyltrimethylammonium bromide (CTAB) (S.D. Fine-Chem, India) and toluene (E-Merck Chemical, India) were procured and used as such.

Preparation of organomodified clay (OMC): A clay sample (2 g) was dispersed in 100 mL water with stirring at room temperature for 8 h and then added 5% aqueous CTAB at room temperature. OMC was washed thoroughly, centrifuged and then dried under freeze-drying.

Preparation of polyethylene clay nanocomposite (PECN) by conventional method: To prepared PECN, a mixing solution process was applied using toluene as solvent. In brief, 0.25 g organo-modified bentonite (OMB) was dispersed in 50 mL toluene with constant stirring at 80 °C in a three-necked round bottomed flask containing a mechanical stirrer and a thermometer. Then separately dissolved 5% LDPE in toluene and added drops to the clay dispersion with constant stirring and

continued for heating for another 2 h. The toluene was distilled off and then solvent was allowed to evaporate completely. Samples were subsequently dried in a vacuum oven for one day at 70 °C and then stored in a desiccator.

Preparation of PECN through exfoliation adsorption using polyethylene-surfactant micelle: An aqueous emulsion of polyethylene-surfactant micelle was prepared by adding water (10 mL) dropwise into a hot toluene solution of CTAB (0.05 g) and polyethylene (1 g) under vigorous stirring. The emulsion was then added dropwise into an aqueous dispersion of organomodified clay (OMC). The mixture was then sonicated for 3 h (20 s on and 40 s off) in an ice-bath. The resulting mixture was washed thoroughly, centrifuged and dried under freeze-drying. The masterbatch solution containing 50% clay was blended with different amounts of polyethylene to prepare PECNs.

Polymer film: A 0.1 mm thickness PECN nanocomposite films were prepared using a die (12 cm × 12 cm). A powdered sample (2 g) was placed within the die and the whole thing was placed between the heated blocks at 120 °C under pressure. After 5 min, die was taken out and after cooling to room temperature and then the film was removed.

Characterization: The X-ray diffraction studies of the samples were carried out to examine the basal spacing of the pure clay and the extent of intercalation in nanocomposites using a Philips X-ray diffractometer using nickel filtered CuK α radiation ($\lambda \sim 0.154$ nm) and operating at 40 kV and 50 mA. A powder form of the sample was used for the XRD experiments. The rheological properties of the prepared nanocomposites were carried out using Anton Paar Physica Modular Compact stress-controlled rheometer (MCR 150) with a parallel plate geometry having 50 mm diameter plates, at a temperature range of 125 to 145 °C. Shear viscosities were measured as a function of shear rates for the molten state of the sample. The dynamic oscillatory measurements were also performed to study the durability of the nanocomposites in the presence of vibration or external stress. Measurements were carried out at angular frequencies varying from 0.1 to 100 rad/s. The dependence of shear viscosity on shear rate was analyzed using rotatory mode. Thermogravimetry (TG) and differential thermal analysis (DTA) were carried out in Shimadzu DTG-60 simultaneous DTA-TG analyzer. The analysis was performed by a dynamic scan in nitrogen at 20 °C/min. The SEM and TEM techniques were employed to examine the fracture surface of the PECN nanocomposite samples. The samples were coated with a thin layer of gold and observed using JEOL JSM 5600 microscope. The Young's modulus and tensile strength of the nanocomposites were measured by following ASTM D638 method. Samples were cut and mechanical testing was carried out in a Model H5KS universal testing machine (UTM) from Tinius Olsen at a crosshead speed of 500 mm/min. The 5 kN (1,000 lbf) single column H5kS has a robust control unit with a backlit LCD positioned for optimum visibility.

RESULTS AND DISCUSSION

Structural characterization: The organo modification of bentonite was carried out using cetyltrimethylammonium

TABLE-1
SAMPLES PREPARED BY ORGANO MODIFICATION OF BENTONITE (OMB)

Sample name	CTAB (%)	Time of stirring (h)	Yield (%)	d-spacing (Å)	Relative intensity	Angle (2θ)
Neat	NA	NA	NA	12.1	100	7.1
OMB-1	10	24	91	14.3	100.00	6.1
OMB-2	20	24	88	16.5	100.00	5.3
OMB-3	20	72	87	74.4	100.00	1.1
OMB-4	30	24	91	22.5	100.00	3.9
OMB-5	40	24	93	46.7	100.00	1.8
OMB-6	43	24	92	18.8	73.89	4.6

bromide (CTAB) in aqueous media. It was observed that foaming of the clay dispersion increased with the amount of surfactant used. The details of surfactant concentrations used in a different organo-modified bentonite (OMB) samples are given in Table-1. Toluene as solvent with varying amounts of OMB, PECNs were prepared by following a ultrasonication method (Table-2). The obtained PECNs were white to light yellow in colour and re-dispersible in non-polar solvents like toluene, xylene, etc.

TABLE-2
DETAILS OF PECN SAMPLES PREPARED

Sample	Clay	Amount of clay (%)	Yield (%)
BEPECTL	Neat	5	97
OBEPE-1	OMB-6	1	95
OBEPE-2	OMB-6	2	99
OBEPE-3	OMB-6	3	98
OBEPE-4	OMB-6	4	96
OBEPE-5	OMB-6	5	95
BEPE-1	OMB-4	5	97
BEPE-2	OMB-3	5	96

FTIR studies: The interaction between the polyethylene-surfactant micelle and silicate layers was confirmed by FTIR spectra where the characteristic peak at 1093 cm^{-1} was found to shift to 1031 cm^{-1} in PECN due to the interaction between the positive charges of the cationic surfactant at micelle surfaces and the negative charges of the silicate surface. The characteristic bands correspond to the pristine bentonite are observed at 3622 cm^{-1} (terminal -OH), 3436 cm^{-1} (-OH *str.* of hydrated water deformation), 1023 cm^{-1} [v(Si-O)], 911 cm^{-1} [δ (Al-OH)] and 525 cm^{-1} [v(Si-O-Al)]. In OMBs, the characteristic peak at 3622 cm^{-1} (-OH terminal) remained intact and the peak at 3436 cm^{-1} is shifted to 3429 cm^{-1} (-OH *str.* of hydrated water deformation), 2919 cm^{-1} , 2846 cm^{-1} [v(C-H)], 1639 cm^{-1} (-OH *str.* of hydrated water deformation) and 1029 cm^{-1} [v(Si-O)].

XRD studies: The extent of intercalation in the nanocomposite was studied using XRD. The patterns of nanocomposites can give evidence for the extent of intercalation/exfoliation of the clay particles in the matrix. A shift to lower angles of the characteristic diffraction peak (d_{001} plane) along the *c*-axis direction of clay suggests an increase in interlayer spacing of the clay, which is referred to as intercalation. The disappearance of the characteristic diffraction peak of clay d_{001} spacing indicates the exfoliation of the clay platelets. A broadening of the peak indicates the partial exfoliation and delaminated clay layers

in the composites. The XRD pattern of organo-modified clays is shown in Fig. 1. With a low amount of CTAB, interlayer spacing (d_{001} plane) of the silicate layer remain intact. As the amount of CTAB increases, another peak in the lower angle appears, which varies with the amount of CTAB.

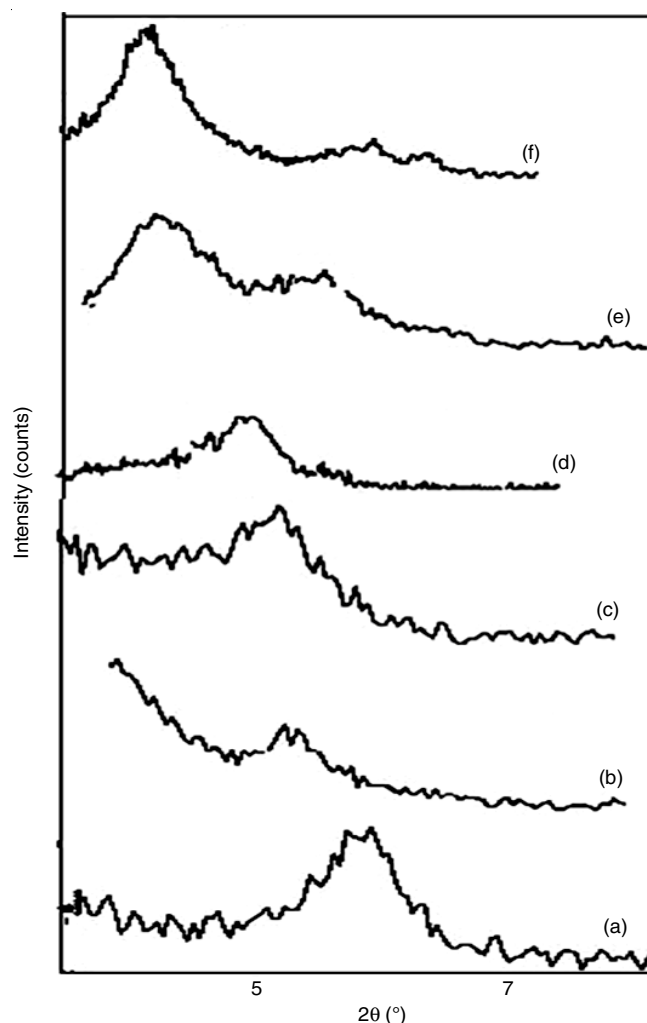


Fig. 1. X-ray diffractogram of different OMB samples [(a) OMB-1, (b) OMB-2, (c) OMB-3, (d) OMB-4, (e) OMB-5, (f) OMB-6]

Fig. 2 shows the typical XRD patterns of bentonite, OMB and PECN samples. Pristine bentonite exhibited characteristic d_{001} basal spacing of 12.1 Å . In PECNs, the d_{001} peak shifted to a lower angle due to the confinement of PE-CTAB micelle into the galleries. The peak shifts to a lower angle depending on

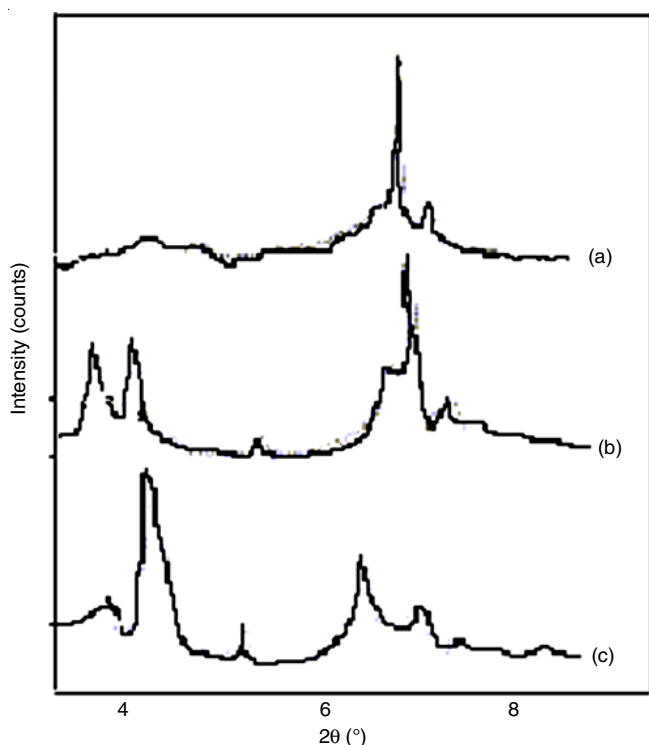


Fig. 2. XRD of (a) PECN, (b) OMB, (c) bentonite

the amount of CTAB and the time of intercalation. Moreover, besides the strong diffraction peak at 4.5° , a weaker diffraction peak was also observed at 6.3° for PECN. This suggested that most of the bentonite layers in PECNs were in the exfoliated/intercalated layered silicate form [26].

Rheological studies: Studies on the oscillatory and rotatory modes reveal the changes in the superstructure of clay platelets in a polymeric matrix under oscillatory and shear stress. The dynamic oscillatory measurements were also performed to measure the durability of the nanocomposites in the presence of external stress. Storage modulus (G') represents the strain energy reversibly stored in the substance, while loss modulus (G'') represents the amount of energy irreversibly given off by the substance. It reveals the linear viscoelastic behaviour with small sinusoidal strain $\gamma(t) = \gamma_0 \sin(\omega t)$. Here γ_0 is the strain amplitude, ω is the frequency and t is real-time. $\tan \delta = G''/G'$ indicates the ratio between the dissipated and the stored energy, *i.e.* the ratio between the viscous and the elastic response of the sample. The magnitude of the complex viscosity is given by $|\eta^*| = \sqrt{(\eta')^2 + (\eta'')^2}$ where η' is the real part of complex viscosity, which stands for the viscous behaviour and η'' is the imaginary part of the complex viscosity, which stands for the elastic behaviour.

The linear viscoelastic response measured by the storage modulus and loss modulus (G' and G'') respectively for various samples were examined as shown in Figs. 3 and 4. These findings explain the influence of OMB content in PECNs on their rheological behaviour. For low clay content in the PECN, only a horizontal (frequency) shift was incorporated as there was no feature present in the moduli data to justify a vertical shift. PECNs with higher OMB content show the vertical modulus shift factor to ascertain a good superposition in the low-frequency

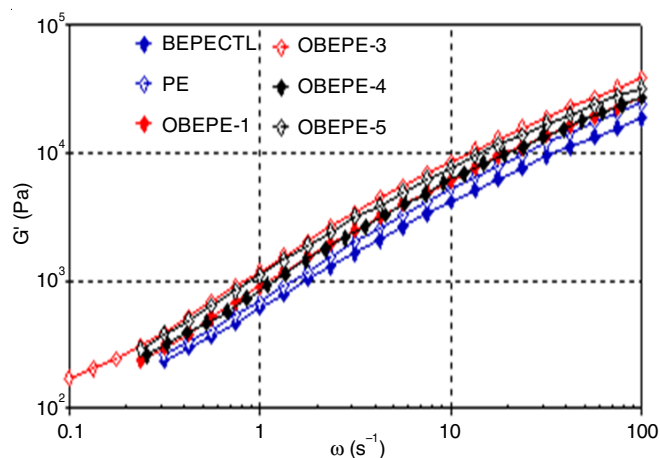


Fig. 3. Storage modulus vs. angular frequency curve for samples with varying OMB content

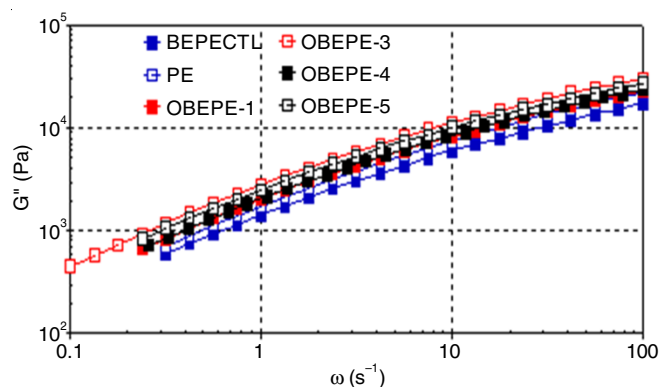


Fig. 4. Loss modulus vs. angular frequency for samples with varying OMB content

regime. For all composites examined, the data was restricted due to the alignment of the silicate layers by applying large amplitude oscillatory shear at low frequencies to obtain the force signals. The storage moduli for the nanocomposite showed a monotonic increase at all frequencies with an increase in silicate content. In case of the loss moduli, the value of polyethylene exceeded that of PECNs. However, the trend for varying wt.% samples suggests that G' increases with an increase in silicate loading.

Terminal zone slopes were estimated for all samples at a frequency below 10 rad/s and are shown in Fig. 5. In close analogy to the PECNs, the terminal zone dependence of G' and G'' for 3-5% samples show non-terminal behaviour with power-law dependence for G' and G'' much smaller than 2 and 1, respectively. The terminal slopes of G' versus G'' curve for PCNs showed a decrease with an increase in clay content. These results indicated that the power-law dependency of PCNs changes inversely with clay concentration. The presence of clay layers and the lack of complete relaxation of chain contribute to this pseudo-solid-like behaviour at the low frequencies, since the storage modulus is less than the loss modulus. This solid-like behaviour is due to forming a percolated network between the silicate layers dispersed in the LDPE matrix. At higher frequencies, this network collapses, resulting in the liquid-like behaviour of the melt. The silicate layers in the hybrids are

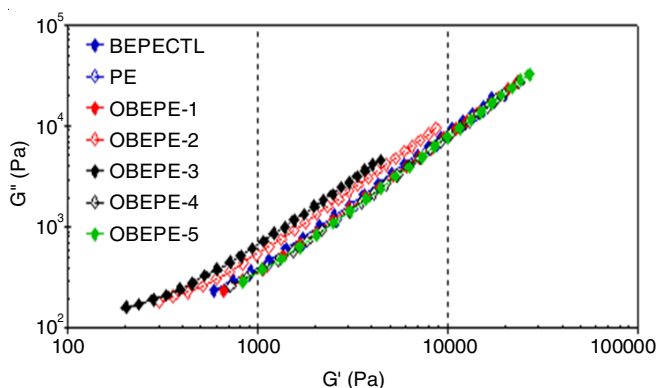


Fig. 5. Storage modulus vs. loss modulus for PECNs with varying OMB content

highly anisotropic with lateral dimensions ranging from 100–1000 nm and even when separated by large dimensions (exfoliated). The plots of log storage modulus (G') vs. log loss modulus (G'') are very useful in investigating the morphological evolution for microphase separated anisotropic phase contained in the nanocomposites. It has been observed that the storage modulus (G') and loss modulus (G'') of OBEPE-5 with 5% OMB content increased to 933 Pa and 2580 Pa, respectively, compared to the G' and G'' values of 685 Pa and 2130 Pa for neat LDPE. This result can be attributed to the change from liquid-like behaviour to solid-like behaviour due to dynamically percolated silicate layers/tactoids.

The higher the storage modulus and the smaller the G'' versus G' curve slope, the more pronounced the interaction between the silicate platelets and their tendency to form a three-dimensional superstructure. Even a small amount of OMB added to the LDPE matrix greatly improved the steady shear viscoelastic response, just like in the dynamic frequency sweep tests. Only at low shear rates were PECN steady shear flow curves close to Newtonian. Similar effects were reported for other filled and mesostructured polymer systems also. This effect can be due to the orientation of silicate layers in the flow direction even in a relatively low shear environment, leading to a domain structure with strong polymer silicate interaction in the PECNs. The higher viscosity exhibited by PECNs compared to LDPE at low shear rates indicates that the flow behaviour of PECNs depends strongly on their matrix and to a lesser extent on the intercalation/exfoliation state of the clay layers. At high shear rates, the LDPE chains start to align in the flow direction, causing the shear-thinning behaviour of viscosity, which accelerates the clay tactoid orientation.

The yield stress is a significant engineering parameter to describe the flow behaviour of several non-Newtonian fluids. A yielding fluid typically shows high Newtonian viscosity at low stresses and a sharp drop in viscosity over a narrow range of shear stress. It was observed that all PECNs showed more or less the same yield stress as LDPE. As shear stress exceeded the apparent yield stress, the structure started to break down, possibly by the incipient alignment of the silicate layers along the flow direction. This caused the material to flow to an increasingly greater extent. PECNs showed a shear-thinning effect at a high shear rate irrespective of the amount of clay, whereas

neat polyethylene exhibited a Newtonian plateau in the melt viscosity measurement. The shear-thinning effect is due to the orientation of the exfoliated nano clay layers in the polymeric matrix. The PECNs showed a strong dependence of viscosity on clay content. The quiescent-state solid-like behaviour and linear stress relaxation behaviour observed for high silicate nanocomposites are conjectured to result from developing a three-dimensional percolated network mesostructure. From the rheological measurements, it can be observed that the BEPECTL (control sample) showed much lower values compared to the LDPE and PECNs. This confirms that there is little or no interaction between LDPE chains and the unmodified clay. The clay particles might be present in the form of aggregates, which adversely affected the properties of the composite.

Effect of clay gallery space on Rheological Behaviour of PECNs: The log storage modulus (G') vs. log loss modulus (G'') for PECN containing OMB having different gallery space is shown in Fig. 6. As an extent of intercalation increases with the gallery space, there can be a significant improvement in the viscoelastic properties for a given weight fraction of OMB. Whereas PECN showed a $\tan \delta$ value of 0.8 at the terminal region of the plot, polyethylene and PECN showed a value of > 2 , as is expected for linear polymers. The low-value PECN is due to the change from liquid-like behaviour to solid-like behaviour attributed to the mesoscopic phase of the superstructure formed by the dispersed aluminosilicate layers/tactoids, resulting in solid-like behaviour analogues to thermotropic liquid crystals. It can be seen that PECNs showed a higher complex viscosity with an increase in OMB gallery space. At higher frequencies (100 rad/s), the viscosity values for OBEPE-5 (d_{001} spacing 46.7) and BEPE-1 (d_{001} spacing 22.5) were the same. This may be due to the incipient alignment of silicate layers in the direction of flow irrespective of the gallery space of the layers. The steady-state viscoelastic properties for PECNs with varying OBE gallery space were studied. The steady shear flow curves were approximately Newtonian at low shear rates. Shear-thinning behaviour was shown in all samples at about 5 s^{-1} and for shear rates higher than that, all the samples showed the same viscosity profile. This suggests that the flow behaviour of PCNs at high shear rates depend solely on the conformational changes in the LDPE matrix.

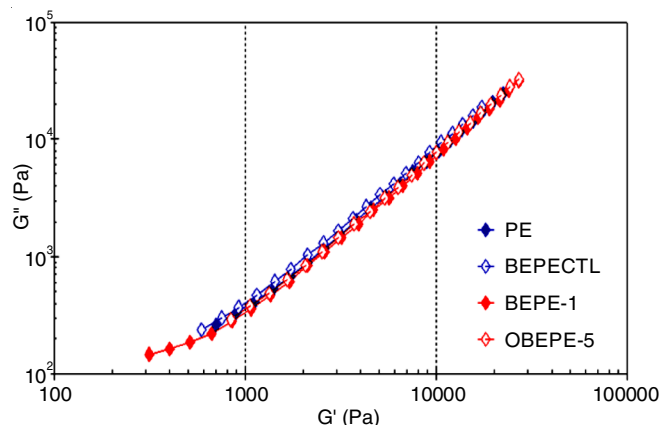


Fig. 6. Storage modulus vs. loss modulus for PECNs with varying OMB gallery space

Effect of temperature on dynamic oscillatory measurements: Effect of temperature on the viscoelastic properties of OBEPE-3 was studied using dynamic oscillatory measurements at angular frequency values between 0.1 and 100 rad/s. Dynamic oscillatory measurements for OBEPE-3 were conducted at 125, 130, 135, 140 and 145 °C. It has been observed that the damping factor ($\tan \delta$) is less than one (< 1) at low frequencies and greater than one (> 1) at higher frequencies confirming solid-like behaviour at low frequencies and liquid-like behaviour at higher frequencies (Fig. 7). At low frequency (0.1 rad/s), storage modulus (G') values converged to 1.7×10^2 Pa. As the angular frequency increased to 1 rad/s, storage modulus values showed substantial differences at different temperatures. It has been observed from the DTA that thermal phase transition is taking place in PECN around 120-130 °C. This might be due to the conformational change exhibited by the intercalated polymer chains inside the clay layers, which affects the guest-host interaction between the clay surface and polymer chain. This observation is quite vivid between angular frequencies 1 and 0.5 rad/s. This can be due to the combined effect of thermal energy and angular frequency, inducing conformational changes of the LDPE and CTAB chains inside the clay layers. The value of G' decreased with an increase in temperature, but at higher frequ-

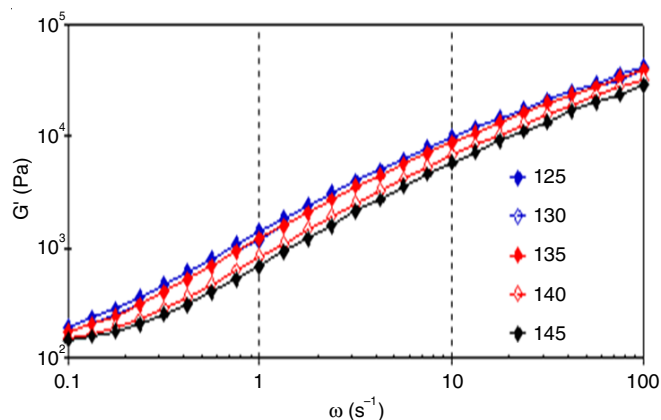


Fig. 7. Temperature dependence of storage modulus for OBEPE-3

encies of the order of 100 rad/s, the G' values again tend to converge to a point. This might be due to the incipient alignment of silicate layers.

Morphological studies: SEM and TEM images of pristine bentonite, LDPE, BEPECTL and OBEPE-5 are shown in Figs. 8 and 9. SEM and TEM studies showed that the morphology of bentonite was observed as a plate-like structure. The SEM image of the LDPE fracture surface shows a ribbon-like texture

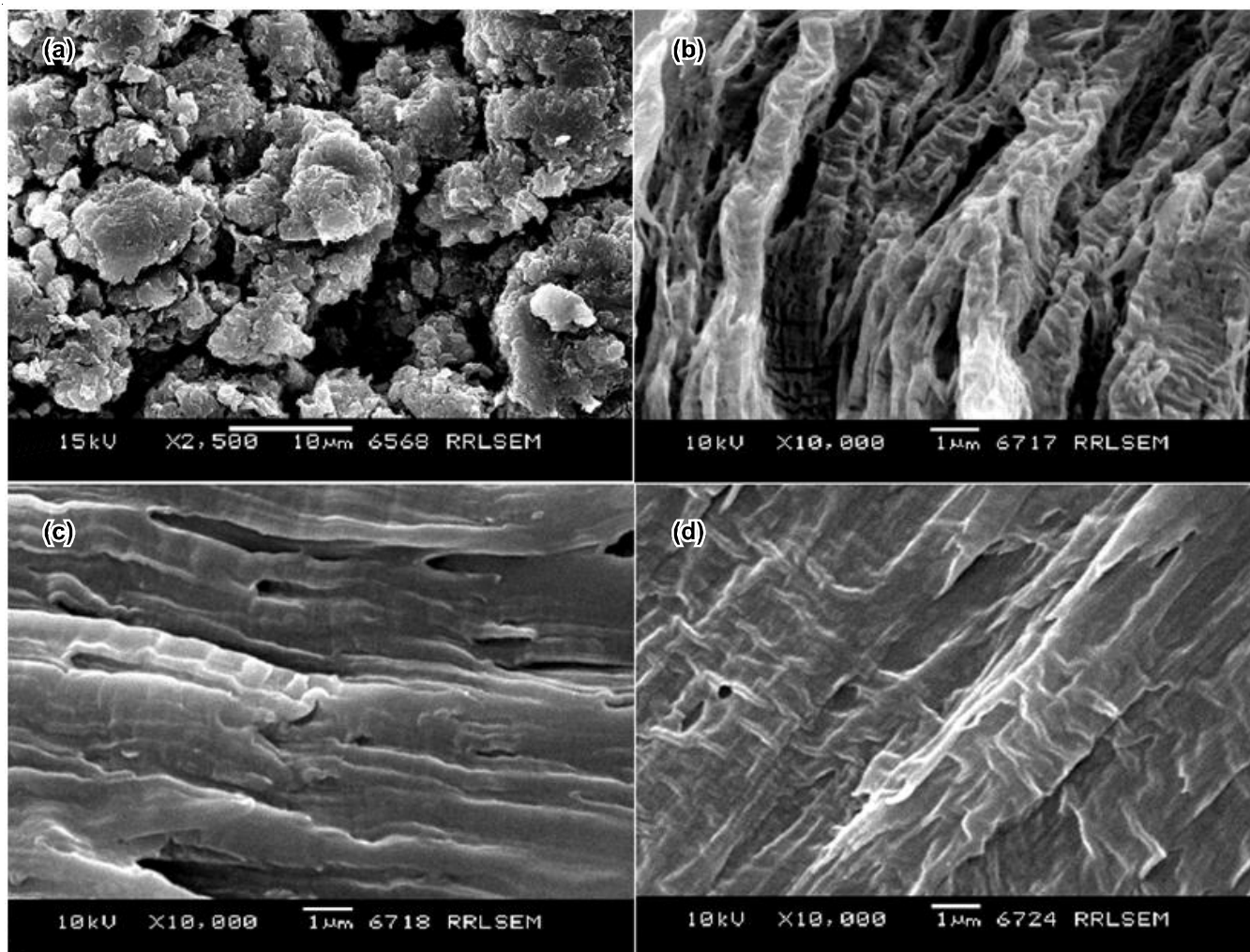


Fig. 8. SEM micrographs of (a) LDPE, (b) bentonite, (c) OBEPE-5, (d) BEPECTL

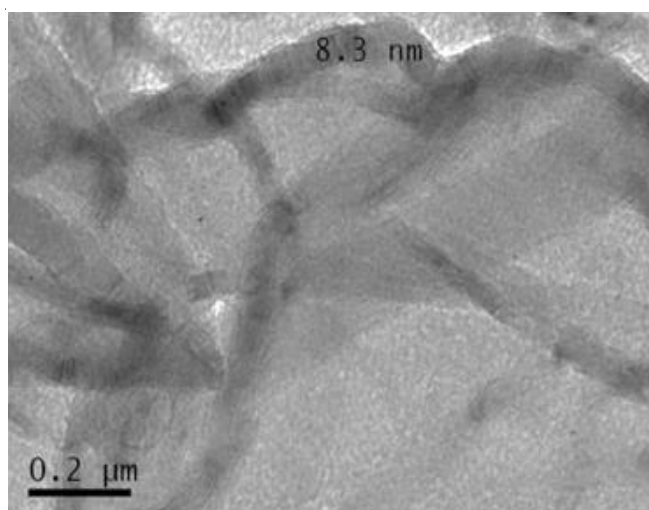


Fig. 9. TEM image of OBEPE

with lots of voids in between the layers. The SEM micrograph of OBEPE-5 (with 5% clay content) exhibited a random bright layers of clay dispersed in the LDPE matrix. In these images, the bright spots on the backscattered images correspond to clay aggregates [27]. A large smooth surface area was observed due to the efficient dispersion and better clay exfoliation in the LDPE matrix. Occasionally some thick tactoids of clay were also observed in the micrograph, confirming the partially exfoliated and partially intercalated silicate layers dispersed in the nanocomposite. Micrograph of BEPECTL, composite of LDPE and clay without organo modification, showed many micro-sized voids. This void can adversely affect the mechanical properties. The fractured surfaces were deformed due to the agglomeration of clay particles in certain regions. This difference is well in agreement with the rheological results for these samples.

Thermal studies: Thermograms data show that PECNs degraded at higher temperatures than LDPE. As the clay content increased, the initial decomposition temperature also increased to 410 °C (OBEPE-1), 412 °C (OBEPE-2), 414 °C (OBEPE-3), 417 °C (OBEPE-4) and 425 °C (OBEPE-5). Char yield of the PECNs is taken at the stabilization stage and matched the amount of clay used for the experiment. This beneficial effect can be explained by a decrease in oxygen and volatile products diffusion throughout the composite material. Moreover, the temperature at which the weight loss is 50% is about 25 °C higher for OBEPE-5 having 5% OMB content. Silicate has a suitable barrier property against the permeation of various atmospheric gases [31]. Thus, the addition of clay enhances the performance of char formed by acting as a superior insulator and mass transport barrier to the volatile products generated during decomposition.

Mechanical testing: Although there is an increase in the values of tensile properties such as Young's modulus and tensile strength, the improvement is not as significant as expected. LDPE exhibited stress at a break of 7.20 MPa and PECNs showed increased values of 7.61 MPa (OBEPE-1), 7.7 MPa (OBEPE-2), 7.9 MPa (OBEPE-3) and 7.79 MPa (OBEPE-4). LDPE exhibited Young's modulus of 0.68 GPa and it increased

to 0.71 GPa when the clay content was increased to 3%. This may be resulting from the debonding between OMB and polyethylene, as explained in microscopic studies. The presence of many micro-sized voids in the SEM pictures is the reason for the lower strength for these nanocomposites than expected. The relatively higher modulus shown by OBEPE-3 with 3% clay content compliments its superior exfoliation as suggested by the rheological measurements.

Conclusion

Polyethylene-clay nanocomposites (PECNs) were prepared by a novel one-pot technique using polyethylene-CTAB micelle by ultrasonication method in an aqueous medium. The rheological behaviour of LDPE and PECNs was studied and the effect of organo-modified bentonite (OMB) content and gallery space on the viscoelastic behaviour of PECNs was studied by dynamic viscoelastic measurements in both oscillatory mode as well as rotatory mode. Rheological behaviour studies indicated the formation of a three dimensional percolated network of the silicate layers and LDPE chains in PECNs. PECNs exhibited pseudo-solid-like behaviour in low-frequency measurements. The SEM of a fractured surface of nanocomposites showed randomly aligned clay tactoids in the polyethylene matrix. Mechanical testing results of PECN showed an increase in the stress at break and Young's modulus. Thermal characterization revealed a significant improvement in the thermal stability for the PECNs prepared through the suggested one-pot method.

ACKNOWLEDGEMENTS

This research was carried out at National Institute for Interdisciplinary Science and Technology CSIR, Thiruvananthapuram, India.

CONFLICT OF INTEREST

The authors declare that there is no conflict of interests regarding the publication of this article.

REFERENCES

1. V.P. Ananikov, *Nanomaterials*, **9**, 1197 (2019); <https://doi.org/10.3390/nano9091197>
2. V. Mittal, *Materials*, **2**, 992 (2009); <https://doi.org/10.3390/ma2030992>
3. A. Usuki, *R&D Review of Toyota CRDL*, **47**, 45 (2016).
4. E. García-Romero, E.M. Manchado, M. Suárez and J. García-Rivas, *Minerals*, **9**, 696 (2019); <https://doi.org/10.3390/min9110696>
5. L. Perelomov, S. Mandzhieva, T. Minkina, Y. Atroshchenko, T. Bauer, I. Perelomova, D. Pinsky and A. Barakhov, *Minerals*, **11**, 707 (2021); <https://doi.org/10.3390/min11070707>
6. P.I. Xidas and K.S. Triantafyllidis, *Eur. Polym. J.*, **46**, 404 (2010); <https://doi.org/10.1016/j.eurpolymj.2009.11.004>
7. S. Mallakpour and M. Dinari, *Appl. Clay Sci.*, **51**, 353 (2011); <https://doi.org/10.1016/j.clay.2010.12.028>
8. S.S. Ray and M. Okamoto, *Progr. Polym. Sci.*, **28**, 1539 (2003); <https://doi.org/10.1016/j.progpolymsci.2003.08.002>
9. T.D. Fomes, P.J. Yoon, D.L. Hunter, H. Keskkula and D.R. Paul, *Polymer*, **43**, 5915 (2002); [https://doi.org/10.1016/S0032-3861\(02\)00400-7](https://doi.org/10.1016/S0032-3861(02)00400-7)
10. S. Gul, A. Kausar, B. Muhammad and S. Jabeen, *Polym. Plast. Technol. Eng.*, **55**, 684 (2016); <https://doi.org/10.1080/03602559.2015.1098699>

11. J. Fawaz and V. Mittal, Eds.: V. Mittal, Synthesis of Polymer Nanocomposites: Review of Various Techniques, In: Synthesis Techniques for Polymer Nanocomposites, Wiley, Chap. 1, pp. 1-30 (2015); <https://doi.org/10.1002/9783527670307.ch1>
12. L. Guadagno, B. De Vivo, A. Di Bartolomeo, P. Lamberti, A. Sorrentino, V. Tucci, L. Vertuccio and V. Vittoria, *Carbon*, **9**, 17 (2011); <https://doi.org/10.1016/j.carbon.2011.01.017>
13. A. Panwar, V. Choudhary and D.K. Sharma, *J. Reinforced Plast. Compos.*, **30**, 446 (2011); <https://doi.org/10.1177%2F0731684411399132>
14. D. Ratna, S. Divekar, A.B. Samui, B.C. Chakraborty and A.K. Banthia, *Polymer*, **47**, 4068 (2006); <https://doi.org/10.1016/j.polymer.2006.02.040>
15. N. Najafi, M.C. Heuzey and P.J. Carreau, *Compos. Sci. Technol.*, **72**, 608 (2012); <https://doi.org/10.1016/j.compscitech.2012.01.005>
16. C. Ou, L. Zhang, Q. Jing, V. Narayan and S. Kar-Narayan, *Adv. Electr. Mater.*, **6**, 1900720 (2020); <https://doi.org/10.1002/aelm.201900720>
17. K.G. Fournaris, M.A. Karakassides, D. Petridis and K. Yiannakopoulou, *Chem. Mater.*, **11**, 2372 (1999); <https://doi.org/10.1021/cm981140z>
18. L. Ludueña, V. Alvarez and V. Analia, *Mater. Sci. Eng. A*, **460-461**, 121 (2007); <https://doi.org/10.1016/j.msea.2007.01.104>
19. C. Çaglayan and T. Güven, *Radiat. Phys. Chem.*, **169**, 107844 (2020); <https://doi.org/10.1016/j.radphyschem.2018.05.003>
20. Q.T. Nguyen and D.G. Baird, *Adv. Polym. Technol.*, **25**, 270 (2006); <https://doi.org/10.1002/adv.20079>
21. Y. Mansoori, S.S. Sanaei, M.-R. Zamanloo, G. Imanzadeh and S.V. Atghia, *Bull. Mater. Sci.*, **36**, 789 (2013); <https://doi.org/10.1007/s12034-013-0542-4>
22. G. Arora and H. Pathak, *Mater. Today Commun.*, **22**, 100829 (2020); <https://doi.org/10.1016/j.mtcomm.2019.100829>
23. R.F. Gibson, *Compos. Sci. Technol.*, **105**, 51 (2014); <https://doi.org/10.1016/j.compscitech.2014.09.016>
24. H. Lee, S. Mall, P. He, D. Shi, S. Narasimhadevara, Y. Yeo-Heung, V. Shanov and M.J. Schulzd, *Compos. B: Eng.*, **38**, 58 (2007); <https://doi.org/10.1016/j.compositesb.2006.04.002>
25. A.M. Díez-Pascual, M.A. Gómez-Fatou, F. Ania and A. Flores, *Prog. Mater. Sci.*, **67**, 1 (2015); <https://doi.org/10.1016/j.pmatsci.2014.06.002>
26. A. Montazeri and N. Montazeri, *Mater. Des.*, **32**, 2301 (2011); <https://doi.org/10.1016/j.matdes.2010.11.003>
27. Y. Wang, L. Shang, P. Zhang, X. Yan, K. Zhang, S. Dou, J. Zhao and Y. Li, *Polym. Test.*, **83**, 106353 (2020); <https://doi.org/10.1016/j.polymertesting.2020.106353>
28. R. Salehiyan, S.S. Ray, J. Bandyopadhyay and V. Ojijo, *Polymers*, **9**, 350 (2017); <https://doi.org/10.3390/polym9080350>
29. M. Kim, H.Y. Song, W.J. Choi and K. Hyun, *Macromolecules*, **52**, 8604 (2019); <https://doi.org/10.1021/acs.macromol.9b01302>
30. Y.M. Zhu, R.M. Cardinaels, J. Mewis and P. Moldenaers, *Rheolog. Acta*, **48**, 1049 (2009); <https://doi.org/10.1007/s00397-009-0387-3>
31. C.M. Wu, W.Y. Hsieh, K.B. Cheng, C.-C. Lai and K.C. Lee, *Nanomaterials*, **8**, 314 (2018); <https://doi.org/10.3390/nano8050314>